Effect of Viscosity on Steady-State Voltammetry and Scanning Electrochemical Microscopy in Room Temperature Ionic Liquids

Kevin R. J. Lovelock, Frances N. Cowling, Alasdair W. Taylor, Peter Licence, and Darren A. Walsh*

School of Chemistry and Faculty of Engineering, University of Nottingham, Nottingham NG7 2RD, United Kingdom

Received: December 22, 2009; Revised Manuscript Received: February 19, 2010

The electrochemical properties of a series of room temperature ionic liquids (RTILs) were studied using voltammetric methods and scanning electrochemical microscopy (SECM). The RTILs consisted of 1-alkyl-3-methylimidazolium cations, $[C_nC_1Im]^+$, and either bis[(trifluoromethyl)sulfonyl]imide anions, $[Tf_2N]^-$, or hexafluorophosphate anions, $[PF_6]^-$. The effect of RTIL viscosity on mass transfer dynamics within each RTIL was studied electrochemically using ferrocene as a redox probe. In the case of the $[C_nC_1Im][Tf_2N]$ RTILs, the viscosity was altered by changing the alkyl chain length. $[C_4C_1Im][PF_6]$ was used for comparison as its viscosity is significantly higher than that of the $[C_nC_1Im][Tf_2N]$ RTILs. The RTIL viscosity affected the ability to record steady-state voltammograms at ultramicroelectrodes (UMEs). For example, it was possible to record steady-state voltammograms at scan rates up to 10 mV s^{-1} in $[C_2C_1Im][Tf_2N]$ using 1.5 μm radius disk UMEs, but non-steady-state behavior was observed at 50 mV s^{-1}. However, at 12.5 μm radius UMEs, steady-state voltammetry was only observed at 1 mV s^{-1} in $[C_2C_1Im][Tf_2N]$. The RTIL viscosity also affected the ability to record SECM feedback approach curves that agreed with conventional SECM theory. In the most viscous $[C_nC_1Im][Tf_2N]$ RTILs, feedback approach curves agreed with conventional theory only when very slow tip approach speeds were used (0.1 μm s^{-1}). These observations were interpreted using the Péclet number, which describes the relative contributions of convective and diffusive mass transfer to the tip surface. By recording feedback approach curves in each RTIL at a range of tip approach speeds, we describe the experimental conditions that must be met to perform SECM in imidazolium-based RTILs. The rate of heterogeneous electron transfer across the RTIL/electrode interface was also studied using SECM and the standard heterogeneous electron transfer rate constant, k^0, for ferrocene oxidation recorded in each RTIL was higher than that determined previously using voltammetric methods.

Introduction

The electrochemical applications of room temperature ionic liquids (RTILs) have grown enormously in recent years and include uses in fuel cell[1,2] batteries[3,4] and photoelectrochemical cells.[5,6] Fundamental electrochemical investigations into mass and charge-transfer dynamics have also been performed using a range of RTILs.[7−9] This work has demonstrated some of the challenges that one faces when attempting to perform electrochemical measurements in RTILs. The effects of ohmic drop must be considered when using RTILs, particularly at large electrodes.[10] Furthermore, due to the relatively high viscosities of most RTILs, diffusion coefficients of redox species are often two or more orders of magnitude lower in RTILs than in conventional solvents, which leads to reduced faradaic currents during voltammetry.[11] The low diffusion coefficients typically encountered in RTILs can also mean that steady-state responses may not be obtained at ultramicroelectrode (UME) surfaces.[12,13] Despite these challenges, a large number of research groups are actively performing electrochemical measurements using RTILs as they provide a unique environment for studying electrochemical phenomena and their prospective applications are increasing enormously.[14−17]

The study of heterogeneous electron transfer (ET) across the electrode/electrolyte interface is particularly important for a wide range of applications and electrochemists have devised a number of methods for measuring the rate of heterogeneous ET. Feedback-mode scanning electrochemical microscopy (SECM), in which the steady-state current, $i_{T,\infty}$, at a μm-sized SECM tip is perturbed by positioning it close to a substrate electrode, is especially useful for studying heterogeneous ET kinetics.[18,19] For a UME positioned far from a substrate surface, the mass transfer coefficient, $m \sim D/a$, where D is the diffusion coefficient of the redox mediator and a is the UME radius. However, when a UME is positioned close (tip-substrate separation of $\sim a$) to a conducting substrate, the mass transfer coefficient, m, becomes a function of the tip-substrate separation, d, and $m \sim D/d$. Therefore, by decreasing d, it is possible to achieve extremely high rates of mass transfer to the tip surface and measure very fast ET kinetics.[20] However, conventional SECM theory, which can be used to obtain kinetic information and to accurately determine the position of the SECM tip relative to the substrate, relies on the ability to record a steady-state current at the SECM tip, and this introduces specific challenges when performing SECM in RTILs. As the diffusion length in a typical SECM measurement is often similar to the distance traveled during SECM feedback approach curve experiments, tip motion can contribute significantly to mass transfer to the tip surface. In sufficiently viscous electrolyte solutions, high tip approach

* Corresponding author. Tel.: +44 115 951 3437. Fax: +44 115 9513562. E-mail: darren.walsh@nottingham.ac.uk.

10.1021/jp912087n
Published on Web 03/12/2010

TABLE 1: Structures of the RTILs Used in this Study

$[C_nC_1Im][Tf_2N]$ (n = 2, 4, 6, 8)	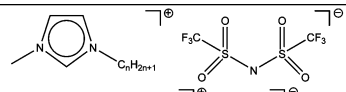
$[C_4C_1Im][PF_6]$	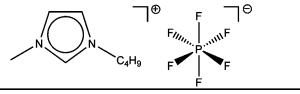

speeds have even yielded positive feedback approach curves at insulating substrates due to enhanced mass transfer caused by motion of the tip.[21,22] Inequalities in the diffusion coefficients of the reduced and oxidized species can also complicate SECM measurements.[23,24] Therefore, due to the difficulties that can arise when attempting SECM experiments in RTILs, some authors have questioned whether SECM can be performed routinely in RTILs.[22]

One of the major advantages of imidazolium-based RTILs is the ability to tune their properties by varying the substituents on the cation and by altering the identity of the anion. In this paper, we describe the electrochemical properties of a series of commonly used 1-alkyl-3-methylimidazolium bis(trifluoromethylsulfonyl)imide-based, $[C_nC_1Im][Tf_2N]$, RTILs, in which the alkyl chain length was altered systematically to vary the RTIL viscosity. A highly viscous RTIL was used for comparison, which was produced by changing the anion from $[Tf_2N]^-$ to $[PF_6]^-$ (Table 1). Cyclic voltammetry and chronoamperometry were used to characterize the mass transfer properties of the RTILs. SECM feedback approach curve experiments were performed in each RTIL, and we demonstrate that, using sufficiently slow tip approach speeds and small SECM tips, it is possible to record feedback approach curves that agree with conventional SECM theory in a range of RTILs. We also used SECM to measure the rate of ET across the electrode/RTIL interface. Significantly, these results show that steady-state SECM yields rate constants that exceed those determined recently in RTILs using methods such as cyclic voltammetry.

Experimental Section

Reagents and Apparatus. All reagents were obtained from Sigma-Aldrich and were used as received, with the exception of 1-methylimidazole, which was dried over CaH_2 and distilled prior to use. RTILs were synthesized according to published procedures[25,26] and were analyzed by ion chromatography (Dionex ICS-3000) before use; in all cases, the halide concentration was <100 ppm. ^1H and ^{13}C NMR spectra were measured on a Bruker DPX-300 spectrometer at 300 and 75 MHz, respectively. All NMR samples were prepared in DMSO-d_6. RTIL viscosities were measured using an Anton-Parr Physica 301 rheometer using a 50 mm parallel plate configuration with a 0.5 mm gap. Water contents were measured using a coulometric Karl Fischer apparatus (Mitsubishi CA100).

Electrochemical Measurements. General electrochemical measurements were performed using a Compactstat Electrochemical Interface (Ivium Technologies, The Netherlands) or an Autolab 30 potentiostat (Eco Chemie B.V., The Netherlands). SECM measurements were performed using a model 910B SECM from CH instruments (Austin, TX). For routine measurements, a 0.55 mm diameter Pt disk working electrode was used, which was polished prior to use using aqueous alumina suspensions (Buehler, Lake Bluff, IL) with decreasing particle sizes (1.0, 0.3, and 0.05 μm) on felt polishing pads. In between each polishing step, the electrode was rinsed with deionized water and sonicated in a small amount of deionized water. The electrode was then dried under a stream of N_2. The counter electrode was a Pt wire and the reference electrode was an RTIL-based $Ag|Ag^+$ electrode, which was described previously,[27] or a silver quasi reference electrode (AgQRE). The formal potential for ferrocene oxidation, $E^{0\prime}$, at the Pt electrode was -0.41 ± 0.01 V versus $Ag|Ag^+$ and $+0.31 \pm 0.01$ V versus AgQRE in the $[C_nC_1Im][Tf_2N]$ RTILs. $E^{0\prime}$ was stable to within a few mV over 8 h when using each reference electrode. All experiments were performed at room temperature and, for consistency, all potentials in the text are reported versus the Fc/Fc^+ couple (except when describing SECM tip voltammogram fitting).

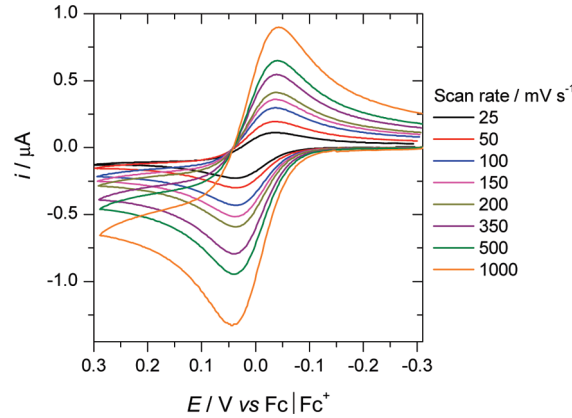

Figure 1. Cyclic voltammograms obtained at a 0.55 mm diameter Pt disk electrode in 4.7 mM Fc in $[C_4C_1Im][Tf_2N]$ at 25, 50, 100, 150, 200, 350, 500, and 1000 mV s^{-1}. The potential was swept between -0.32 V and $+0.28$ V vs $Fc|Fc^+$ and the initial potential was -0.32 V.

Pt disk (radius 12.5 μm) UMEs were constructed by heat sealing Pt microwire (25 μm diameter, Goodfellow, U.K.) into soft glass using a similar procedure to that reported previously.[28] SECM tips were prepared by heat sealing a 25 μm diameter Pt wire into a quartz capillary tube and pulling the capillary to a fine point using a laser micropipet puller (Model P2000, Sutter Instrument co., Novato, CA) under vacuum ($\sim 10^{-2}$ mbar), as described previously.[29] The Pt was exposed and the tip was sharpened using a microelectrode beveller (Sutter Model BV-10). SECM tips (radius 1.5 μm) were used with average RG values ($RG = r_g/a$, where r_g is the radius of the insulating glass sheath) of approximately 10 (estimated using optical microscopy). Prior to use, the radius and geometry of the SECM tips were confirmed using cyclic voltammetry and SECM feedback approach curve experiments in 1 mM ferrocenemethanol dissolved in 0.1 M aqueous KCl. In between measurements, the SECM tip surface was gently polished using the microelectrode beveller.

Results and Discussion

Diffusion of Ferrocene in RTILs. Figure 1 shows typical cyclic voltammograms recorded at various scan rates in 4.7 mM ferrocene (Fc) dissolved in $[C_4C_1Im][Tf_2N]$. The ratio of the anodic peak current, $i_{p,a}$, to the cathodic peak current, $i_{p,c}$, was close to 1 at all scan rates. In addition, $i_{p,a}$ and $i_{p,c}$ were proportional to $v^{1/2}$, where v is the voltammetric scan rate, indicating that mass transfer of Fc to the electrode surface was diffusion controlled. CVs recorded for Fc oxidation in $[C_2C_1Im][Tf_2N]$, $[C_6C_1Im][Tf_2N]$, and $[C_8C_1Im][Tf_2N]$ gave similar responses, that is, $i_p \propto v^{1/2}$ and $i_{p,a}/i_{p,c} \approx 1$. ΔE_p, the separation between the anodic peak potential and the cathodic peak potential was greater than 59 mV at all scan rates and increased as v increased in each RTIL, suggesting that sluggish ET kinetics or ohmic resistance influenced the voltammetric

TABLE 2: D_{Fc} and D_{Fc}^+ in each RTIL and the Viscosity and H_2O Content of Each RTIL[a]

RTIL	10^7 D_{Fc}/cm^2 s^{-1}	10^7 D_{Fc}^+/cm^2 s^{-1}	η/mPa s^{-1}	H_2O/ppm
$[C_2C_1Im][Tf_2N]$	3.7 ± 0.09	3.4 ± 0.08	27	5270
$[C_4C_1Im][Tf_2N]$	3.1 ± 0.06	2.4 ± 0.05	43	4040
$[C_6C_1Im][Tf_2N]$	2.2 ± 0.05	1.6 ± 0.04	59	4250
$[C_8C_1Im][Tf_2N]$	1.8 ± 0.04	1.9 ± 0.04	84	600
$[C_4C_1Im][PF_6]$	0.7 ± 0.01	0.7 ± 0.01	203	1550

[a] η was determined using rheometry and the H_2O content was determined using Karl Fischer titrations. D_{Fc} and D_{Fc}^+ were determined using chronoamperometry at a 0.55 mm diameter Pt disk electrode.

response in each RTIL. The sluggishness of ET across the electrode/RTIL interface is dealt with in a later section. Double potential step chronoamperometry was used to determine the diffusion coefficients of the reduced and oxidized forms of Fc, D_{Fc} and D_{Fc}^+, in each RTIL. A representative $i-t$ transient obtained during chronoamperometric Fc oxidation and reduction in $[C_4C_1Im][Tf_2N]$ is shown in Figure S1A in the Supporting Information and Figure S1B shows typical Cottrell plots (i vs $t^{-1/2}$) for each branch of the chronoamperogram. D_{Fc} and D_{Fc}^+ were obtained from the slopes of the best-fit lines fit to the Cottrell plots (and using the Cottrell equation) and are shown in Table 2 for each RTIL. Table 2 also shows the water content of each RTIL, as measured by Karl Fischer titration, and the viscosity of each RTIL as measured using rheometry. The viscosity of each RTIL was slightly (10−20%) lower than the literature value,[30] due to the water present in each RTIL.[31] D_{Fc} and D_{Fc}^+ were similar in magnitude to values previously reported for Fc in $[C_nC_1Im][Tf_2N]$ RTILs.[11,32] In general, D_{Fc} and D_{Fc}^+ decreased with increasing RTIL viscosity (with the exception of D_{Fc}^+ on going from $[C_6C_1Im][Tf_2N]$ to $[C_8C_1Im][Tf_2N]$). In addition, in $[C_2C_1Im][Tf_2N]$, $[C_4C_1Im][Tf_2N]$ and $[C_6C_1Im][Tf_2N]$, D_{Fc} was higher than D_{Fc}^+, as has also been observed previously in RTILs[32] and which is due to the increased interactions between the positively charged Fc^+ and the RTIL. We also determined D_{Fc} and D_{Fc}^+ in $[C_4C_1Im][PF_6]$, which is significantly more viscous than any of the $[Tf_2N]^-$-containing RTILs (Table 2). D_{Fc} and D_{Fc}^+ were almost an order of magnitude smaller in $[C_4C_1Im][PF_6]$ than in $[C_4C_1Im][Tf_2N]$, which demonstrates the effect of changing the anion on the RTIL viscosity and, consequently, on the diffusion coefficient of dissolved redox species. Figure S2 in the Supporting Information shows a graph of D_{Fc} versus $1/\eta$, which was reasonably linear for the range of RTIL viscosities studied, indicating that the Stokes−Einstein relationship holds in these RTILs, at least in the sense that D_{Fc} was proportional to $1/\eta$ (the least-squares correlation coefficient, $R^2 = 0.94$).[33] This indicates that the hydrodynamic radius of Fc did not change significantly with changes in the RTIL viscosity. In addition, the hydrodynamic radius of Fc was calculated from the slope of the best-fit line in Figure S2 and was 2.4 Å, which is close to the crystallographic radius of 2.7 Å.[34]

Ultramicroelectrode Voltammetry in RTILs. Before undertaking any measurements using SECM, it is important to verify that one can record steady-state voltammograms at UMEs. In this section, we describe the effect of altering the RTIL viscosity on the voltammetric response obtained at UMEs. The condition for steady-state voltammetry at UMEs is that $v \ll RTD/nFa^2$, where R is the gas constant, T is the temperature, n is the number of electrons transferred during the reaction, and F is the Faraday constant.[35] Therefore, at a 12.5 μm radius UME, one may only expect to obtain steady-state voltammograms during Fc oxidation in $[C_4C_1Im][PF_6]$ when $v \ll 1$ mV s^{-1}. However, at a 1.5 μm radius UME, one may expect steady-state currents at $v \ll 80$ mV s^{-1}. Figure 2A shows voltammograms recorded at a 12.5 μm radius Pt disk UME during Fc oxidation at $v = 1$, 10, and 50 mV s^{-1} in $[C_4C_1Im][PF_6]$ (in which $D_{Fc} = 7 \times 10^{-8}$ cm^2 s^{-1}). Peak-shaped responses were obtained at each scan rate, which were indicative of linear diffusion to the electrode surface. This is in agreement with the expected behavior described above, which shows that steady-state behavior should be observed only when $v \ll 1$ mV s^{-1}. Figure 2B shows the responses obtained in $[C_2C_1Im][Tf_2N]$, which is significantly less viscous than $[C_4C_1Im][PF_6]$ ($D_{Fc} = 3.7 \times 10^{-7}$ cm^2 s^{-1} in $[C_2C_1Im][Tf_2N]$). In this RTIL, steady-state behavior should be observed at $v \ll 6$ mV s^{-1} at a 12.5 μm UME and Figure 2B shows that approximately steady-state behavior was observed only at $v = 1$ mV s^{-1}, but as the scan rate increased, peak-shaped responses were obtained, demonstrating that linear diffusion dominated at higher scan rates. As discussed above, steady-state responses should be observed at $v \ll 80$ mV s^{-1} at a 1.5 μm radius UME in $[C_4C_1Im][PF_6]$, and Figure 2C shows the responses obtained at a 1.5 μm UME at 1, 10, and 50 mV s^{-1} in $[C_4C_1Im][PF_6]$. Steady-state, scan-rate independent responses were observed at $v < 10$ mV s^{-1}. The steady-state currents obtained at 1 and 10 mV s^{-1} were within 1 pA of each other; the current at 1 mV s^{-1} was 21 pA and the current at 10 mV s^{-1} was 20 pA. This difference is insignificant under our experimental conditions and is most likely due to slight differences in the tip conditions from one experiment to another. However, when $v = 50$ mV s^{-1}, more peak-shaped responses were obtained, demonstrating that, as the voltammetric scan rate approached 80 mV s^{-1}, linear diffusion became significant, in agreement with the expected behavior.

In the case of $[C_2C_1Im][Tf_2N]$, steady-state responses should be obtained at $v \ll 400$ mV s^{-1} at a 1.5 μm UME. Figure 2D shows that the currents at 1, 5, and 10 mV s^{-1} agreed with each other to within 2 pA. The current at 1 mV s^{-1} (53 pA) was slightly higher than that obtained at 5 and 10 mV s^{-1} (each was 51 pA), which again is within the experimental error of our measurement. Therefore, we conclude that during Fc oxidation in $[C_2C_1Im][Tf_2N]$, steady-state currents can be measured at scan rates ≤ 10 mV s^{-1}. However, the steady-state current recorded at 50 mV s^{-1} (58 pA) was higher than that recorded at 1, 5, or 10 mV s^{-1}. In addition, the shape of the CV changed quite significantly at 50 mV s^{-1} and we believe that these changes are significant and that, even at 50 mV s^{-1}, which is $\ll$400 mV s^1, non-steady state current may have contributed to the measured current. These results clearly show that, when performing voltammetry at UMEs in RTILs, the response that one obtains depends very strongly on the experimental conditions, as has also been demonstrated in previous work.[12] One must take great care when choosing the UME dimensions, the voltammetric scan rate and the particular RTIL to record a true steady-state current. As we demonstrate in the following section, the experimental parameters also impact quite significantly on the ability to record SECM feedback approach curves in different RTILs.

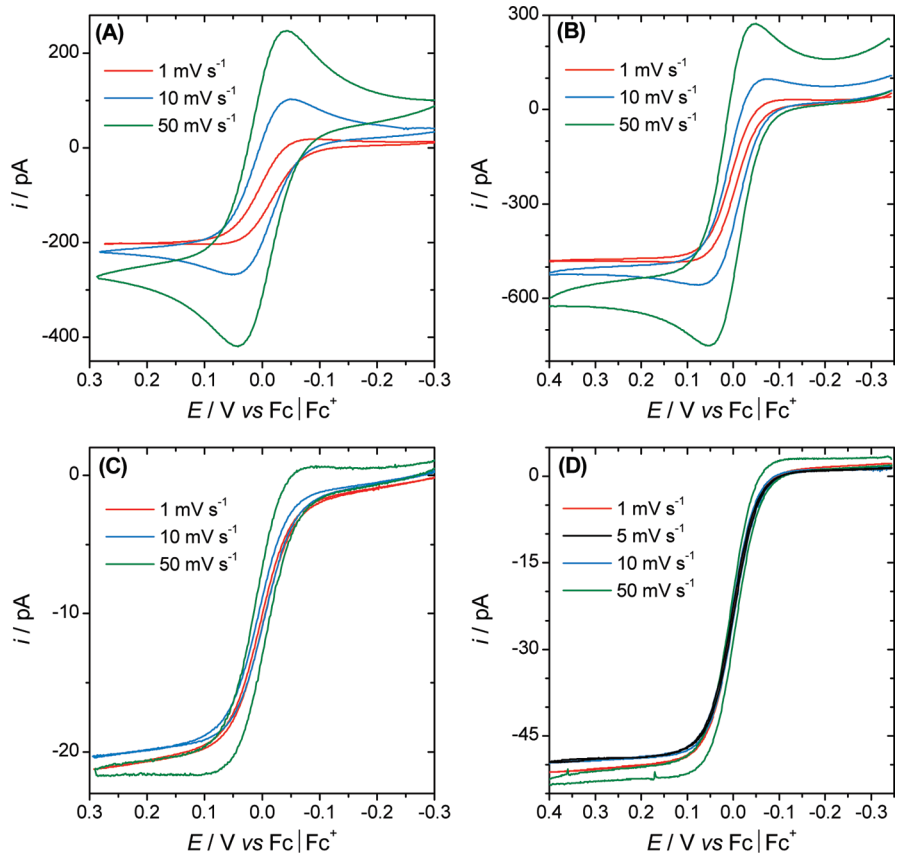

Figure 2. Cyclic voltammograms obtained at a 12.5 μm radius Pt disk UME in (A) 3.20 mM Fc in $[C_4C_1Im][PF_6]$ and (B) 1.56 mM Fc in $[C_2C_1Im][Tf_2N]$. (C and D) Responses obtained at a 1.5 μm radius Pt disk UME in 3.20 mM Fc in $[C_4C_1Im][PF_6]$ and 1.56 mM Fc in $[C_2C_1Im][Tf_2N]$, respectively. The voltammetric scan rates were 1, 10, and 50 mV s^{-1} and additionally 5 mV s^{-1} for (D).

Scanning Electrochemical Microscopy in RTILs. As discussed previously, the low diffusion coefficients typically observed in RTILs can cause difficulties when attempting to perform SECM.[12] Convection caused by movement of the tip can contribute significantly to mass transfer to the tip surface and produce anomalous effects such as increases in i_T as the tip approaches insulating surfaces.[21,22] These complications can make it very difficult to determine the position of the SECM tip relative to the substrate, which is very important when performing kinetic measurements using the SECM. Therefore, it is important to understand the contributions of convection and diffusion to the tip surface during SECM experiments and, in this section, we discuss the parameters that affect the ability to record approach curves that agree with conventional SECM theory in imidazolium-based RTILs. Figure 3 shows approach curves recorded in a range of RTILs using an insulating substrate and a range of tip approach speeds, v_0. Also shown in each part of Figure 3 is the theoretical negative feedback approach curve determined using eq 1 for a tip with RG = 10.[36] Note that a theoretical curve for a tip with RG = 8 was used in one case, which changes the coefficients used in eq 1; see ref 36 for details.

$$i_T/i_{T,\infty} = \frac{1}{\left[0.40472 + \frac{1.60185}{L} + 0.58819\exp\left(\frac{-2.37294}{L}\right)\right]} \quad (1)$$

$i_{T,\infty}$ is the steady-state current at the SECM tip when positioned very far from a substrate surface and L is the normalized tip-substrate separation ($L = d/a$, where d is the distance between the tip and the substrate). Figure 3A shows negative feedback approach curves obtained during Fc oxidation in $[C_4C_1Im][PF_6]$. At each v_0 value, poor agreement between the experimental curve and the theoretical curve was observed. At the highest v_0 values (4 and 8 μm s^{-1}), i_T was actually higher than $i_{T,\infty}$ over a wide range of L. This enhancement in i_T was not due to positive feedback of Fc^+ from the substrate (which was an insulator), but was due to convective mass transfer due to tip movement.[21,22] At sufficiently slow tip approach speeds (e.g., 0.05 μm s^{-1}), the feedback approach curve almost agreed with the theoretical response but i_T was still slightly higher than that predicted by theory at almost all L values. The relative contributions of convective mass transfer and diffusive mass transfer to the SECM tip can be estimated using the Péclet number, Pe:[21]

$$\mathrm{Pe} = \frac{v_0 a}{D} \quad (2)$$

LeSuer has investigated the effects of different Pe numbers on the shape of SECM feedback approach curves obtained in deep eutectic solvents and shown that, when Pe $\leq$ 0.01, convection effects are negligible and feedback approach curves should fit conventional theory.[21] The estimated Pe values for the feedback approach curves shown in Figure 3A ranged between 1.7 and 0.011 (Table S1 in the Supporting Information) and, even at the smallest Pe values, the approach curves did not fit conventional SECM theory.

Figure 3B−D shows SECM feedback approach curves obtained during Fc oxidation in the less viscous RTILs

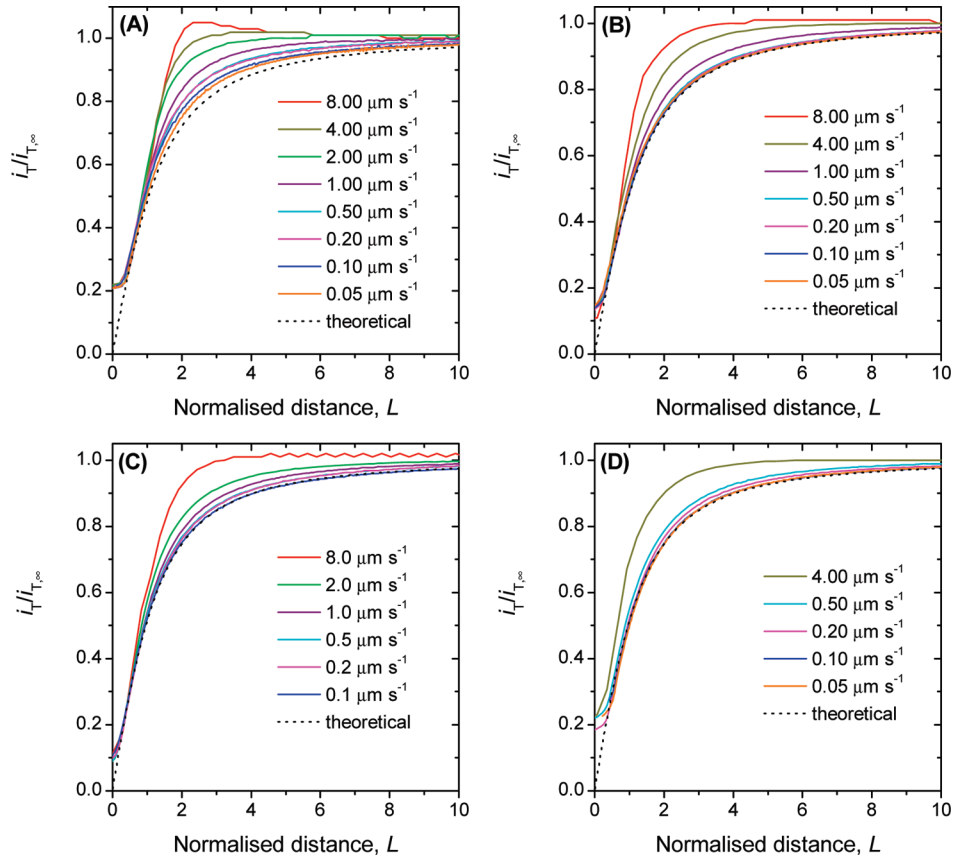

Figure 3. Feedback approach curves obtained in (A) 3.20 mM Fc in $[C_4C_1Im][PF_6]$, (B) 3.50 mM Fc in $[C_4C_1Im][Tf_2N]$, (C) 3.30 mM Fc in $[C_6C_1Im][Tf_2N]$, and (D) 4.35 mM Fc in $[C_8C_1Im][Tf_2N]$ as a 1.5 μm SECM tip approached a PTFE substrate. The tip was held at (A) +0.43 V, (B) +0.47 V, (C) +0.38 V, and (D) +0.38 V vs $Fc|Fc^+$. In each case, the dashed line shows the theoretical negative feedback approach curve generated for an SECM tip with $RG = 10$ ($RG = 8$ in D).

$[C_4C_1Im][Tf_2N]$, $[C_6C_1Im][Tf_2N]$ and $[C_8C_1Im][Tf_2N]$ as a 1.5 μm SECM tip approached an insulating surface. At high v_0 values (1−8 μm s^{-1}) in $[C_4C_1Im][Tf_2N]$, the feedback approach curves did not fit the theoretical negative feedback approach curve (Figure 3B). However, at smaller v_0 values (0.05−0.5 μm s^{-1}), the experimental feedback approach curves fit the theoretical curve very well. This demonstrates that convective mass transfer effects are negligible in this RTIL using the 1.5 μm tip at relatively low v_0 (the approach curves recorded at the 5 slowest tip approach rates in Figure 3B all overlap with each other). The calculated Pe values for $v_0 = 0.05-0.5$ μm s^{-1} are 0.0025−0.025 (Table S1 in the Supporting Information). Therefore, a maximum Pe value of ≈0.025 is required to obtain SECM feedback approach curves that fit conventional SECM theory in $[C_4C_1Im][Tf_2N]$. This is close to the value at which convective effects should be negligible according to LeSuer (Pe ≈ 0.01).[21] Figures 3C and 3D, which show approach curves recorded in $[C_6C_1Im][Tf_2N]$ and $[C_8C_1Im][Tf_2N]$, demonstrate the effect of increasing the RTIL viscosity on the ability to record feedback approach curves that agree with conventional theory. In each of these RTILs, tip approach speeds of about 0.1 μm s^{-1} were necessary to ensure that convective effects were negligible. This clearly demonstrates that, as the RTIL viscosity increases, the tip approach speed must be reduced accordingly to eliminate convective effects during feedback approach curve experiments. Table 3 contains the highest v_0 values at which feedback approach agreed with conventional SECM theory in each RTIL and the associated experimental parameters. A full description of the experimental parameters used in all approach experiments is given in Table S1 in the Supporting Information, which also describes the Pe values at which the feedback approach did and did not agree with SECM theory. Also included in Table S1 is the data from previous studies in which SECM feedback approach curves were recorded in RTILs and whether the curves fit conventional SECM theory. For example, we recently recorded feedback approach curves in solutions of the ferrocenylated RTIL 1-ferrocenylmethyl-3-methylimidazolium $[Tf_2N]^-$ dissolved in $[C_2C_1Im][Tf_2N]$; the calculated Pe value is 0.015 and the approach curve fitted conventional SECM theory.[29] The data in Tables 3 and S1 reveal slight differences in the upper limits of Pe at which approach curves agreed with conventional SECM theory. For example, feedback approach curves did not fit theory when Pe = 0.015 in $[C_6C_1Im][Tf_2N]$ but did fit when Pe = 0.0075. However, in $[C_4C_1Im][Tf_2N]$, the approach curve agreed with theory when Pe = 0.025. In addition, the approach curves did not fit conventional SECM

TABLE 3: Maximum Pe Values (and Associated Experimental Parameters) at which Approach Curves Agreed with Conventional SECM Theory in Each RTIL[a]

RTIL	v_0/μm s^{-1}	a/μm	D/cm^2 s^{-1}	Pe
$[C_4C_1Im][PF_6]$	0.05	1.5	7×10^{-8}	(0.011)[b]
$[C_2C_1Im][Tf_2N]$	0.1	1.5	4×10^{-7}	0.0038
$[C_4C_1Im][Tf_2N]$	0.5	1.5	3×10^{-7}	0.025
$[C_6C_1Im][Tf_2N]$	0.1	1.5	2×10^{-7}	0.0075
$[C_8C_1Im][Tf_2N]$	0.1	1.5	2×10^{-7}	0.0075

[a] Pe values were determined using eq 2 in the text. Table S1 in the Supporting Information contains an expanded data set, which shows the entire range of experiments carried out and the associated Pe values. [b] This Pe value was the minimum obtained in $[C_4C_1Im][PF_6]$, but the feedback approach curve still did not agree with conventional SECM theory.

theory in $[C_4C_1Im][PF_6]$, even at Pe = 0.011. We believe that these differences may be due to errors in estimating D_{Fc}, which may lead to overestimations or underestimations of Pe. Nonetheless, we can conclude that a Pe value of ≈0.01−0.02 is generally required to obtain feedback approach curves that agree with theory. LeSuer has reported previously that when Pe > 1, convective effects cannot be ignored. However, our results demonstrate that, in the range 0.01 ≤ Pe ≤ 1, convective effects can hinder the ability to record SECM feedback approach curves, which agree with conventional SECM theory, in imidazolium-based RTILs. LeSuer has also published theoretical feedback approach curves that incorporate convective effects into the model.[21] However, the Pe values in all of the experiments described here were outside the range of the published working curves (1.75 ≤ Pe ≤ 5). Therefore, we cannot fit our approach curves to the published theoretical curves that incorporate convective effects but we are currently studying RTIL systems with higher Pe values to explore the effects on SECM feedback approach curves.

In summary, we have shown here it is possible to record SECM feedback approach curves that agree with conventional SECM theory in a range of imidazolium-based RTILs. However, one must always take care when choosing the SECM tip and it is likely that reasonably small (<2 μm) tips will be required for even the least viscous of RTILs. In addition, one must ensure that the effect of the tip approach speed is understood and Pe provides a very useful guide for designing SECM experiments in RTILs.

Heterogeneous Electron Transfer Kinetics across the RTIL/Electrode Interface. We recently described the use of SECM in studying the kinetics of heterogeneous electron transfer kinetics across the RTIL/electrode interface.[29] In that study, the heterogeneous electron transfer rate constant, k^0, determined using SECM exceeded that determined using cyclic voltammetry. This suggests that ohmic effects may affect the ability to obtain accurate kinetic data in RTILs using CV. Indeed, others have also suggested that uncompensated *iR* drop may complicate the determination of accurate kinetic data in RTILs and that k^0 values determined using voltammetry in RTILs should at best be considered "apparent" values.[37,38] Steady-state SECM is an extremely useful method for determining accurate kinetic data as it eliminates ohmic effects and problems associated with adsorption of reactants and charging currents.[39] Mirkin and coworkers have measured k^0 for a range of redox species in aqueous and nonaqueous electrolytes using steady-state SECM at nanoscopic SECM tips and, in some cases, obtained higher k^0 values than those previously obtained using other electrochemical methods.[20,40] In this section, we describe the use of steady-state SECM for measuring k^0 in $[C_2C_1Im][Tf_2N]$, $[C_4C_1Im][Tf_2N]$, $[C_6C_1Im][Tf_2N]$, and $[C_8C_1Im][Tf_2N]$ and compare the results with data from the recent literature. As described above, we could not obtain feedback approach curves that agreed with SECM theory in the most viscous RTIL studied ($[C_4C_1Im][PF_6]$) using reasonable tip approach speeds. This makes it difficult to calculate the distance between the tip and the substrate in this RTIL. It is likely that much smaller (nanoscopic) SECM tips will be necessary to perform SECM measurements in such highly viscous RTILs and, due to these complications, we did not attempt any kinetic measurements in $[C_4C_1Im][PF_6]$.

Before one performs kinetic measurements using the SECM, it is important that the SECM tip dimensions and geometry are characterized fully. Figure 4 shows positive and negative feedback approach curves obtained during Fc oxidation in

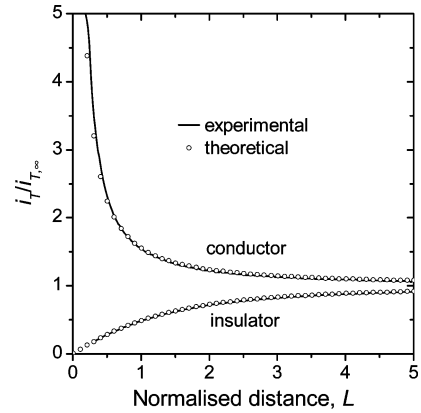

Figure 4. Approach curves obtained during the oxidation of 1.56 mM Fc in $[C_2C_1Im][Tf_2N]$ as a 1.5 μm SECM tip approached a PTFE substrate (lower curve) and a 2 mm Pt disk substrate (upper curve). The tip was held at +0.45 V vs $Fc|Fc^+$ and the tip approach rate was 0.1 μm s^{-1} in each case. Experimental curves are shown by the solid lines and theoretical curves generated for a 1.5 μm tip with $RG = 10$ are shown by the open circles. During the approach to the Pt substrate, the substrate potential was held at −0.2 V vs $Fc|Fc^+$.

$[C_2C_1Im][Tf_2N]$ as a 1.5 μm tip approached conducting and insulating surfaces. Also shown are the theoretical positive and negative feedback approach curves for a tip with RG = 10, which were determined using eqs 1 (above) and 3, respectively:[36]

$$i_T/i_{T,\infty} = 0.68 + \frac{0.78377}{L} + 0.3315\exp\left(\frac{-1.0672}{L}\right) \quad (3)$$

Excellent agreement between the experimental and theoretical curves was observed in each case, which is perhaps unsurprising as Pe = 0.0038 in these experiments. The agreement between the experimental and theoretical curves also indicates that our estimate of the RG value using optical microscopy was accurate. In addition, the best fits to both curves yielded a tip radius of 1.5 μm, as also estimated using optical microscopy.

Mirkin recently developed the following approximate equation for calculating i_T when finite ET kinetics dominate at the tip and the substrate reaction is diffusion controlled:[20]

$$I_T(E,L) = \frac{0.78377}{L(\theta + 1/\kappa)} + \frac{0.68 + 0.3315\exp(-1.0672/L)}{\theta\left[1 + \frac{\pi}{\kappa\theta}\frac{2\kappa\theta + 3\pi}{4\kappa\theta + 3\pi^2}\right]} \quad (4)$$

where $I_T(E,L)$ is the normalized tip current at potential E and normalized distance L above the substrate, $\theta = 1 + \exp[F(E^{0\prime} - E)/RT]D_O/D_R]$, $\kappa = \pi\lambda\exp[F(1-\alpha)(E - E^{0\prime})/RT]/(4I_T^c)$, α is the transfer coefficient, $E^{0\prime}$ is formal potential, $\lambda = k^0a/D$ and k^0 is the standard heterogeneous electron transfer rate constant. I_T^C is the normalized diffusion limiting tip current at the same distance L above a conducting substrate, which is given by eq 3 above. $I_T(E,L)$ is normalized by the steady-state diffusion limited current at a disk UME far from the substrate:

$$i_{T,\infty} = 4nFDCa \quad (5)$$

A 1.5 μm SECM tip was positioned at a range of distances above a 2 mm radius Pt disk substrate and tip CVs for Fc oxidation were recorded in each RTIL. For example, Figure 5

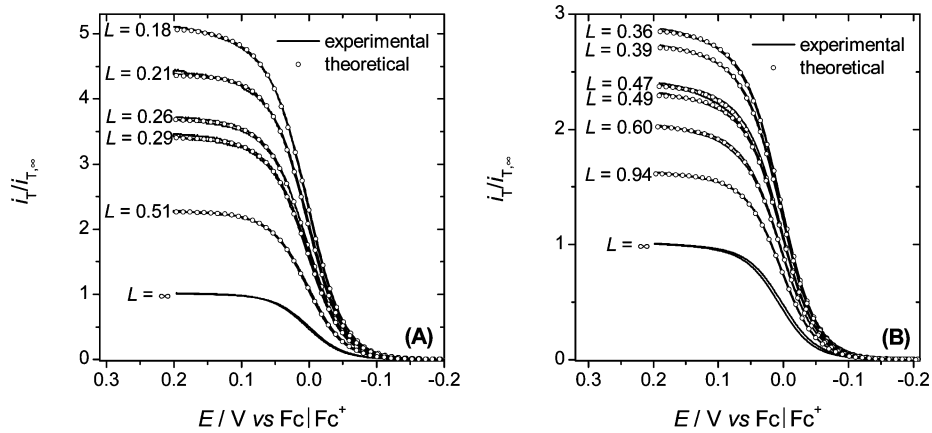

Figure 5. Experimental voltammograms (solid lines) obtained at a 1.5 μm radius Pt UME tip at various normalized distances from a 2 mm diameter Pt disk substrate. (A) Responses obtained in 1.56 mM Fc in $[C_2C_1Im][Tf_2N]$. (B) Responses obtained in 3.30 mM Fc in $[C_6C_1Im][Tf_2N]$. In each case, the tip potential was swept between −0.2 and +0.2 V vs $Fc|Fc^+$ at 5 mV s^{-1} and the substrate potential was −0.2 V vs $Fc|Fc^+$. The theoretical voltammograms at each distance (open circles) were calculated using eq 4.

TABLE 4: Kinetic Parameters for Fc Oxidation at 1.5 μm Radius Pt SECM Tips at Various L Values[a]

RTIL	L	k^0/ cm s^{-1}	α	$E^{0\prime}$/ V vs $Ag\|Ag^+$	λ' or λ
$[C_2C_1Im][Tf_2N]$	0.17	0.078	0.61	−0.405	5.4
$[C_2C_1Im][Tf_2N]$	0.18	0.072	0.57	−0.406	5.3
$[C_2C_1Im][Tf_2N]$	0.21	0.097	0.40	−0.406	8.3
$[C_2C_1Im][Tf_2N]$	0.29	0.065	0.45	−0.406	7.6
$[C_2C_1Im][Tf_2N]$	0.51	reversible		−0.406	16.1
$[C_2C_1Im][Tf_2N]$	∞	reversible		−0.406	30.8
$[C_4C_1Im][Tf_2N]$	0.25	0.041	0.53	−0.422	5.0
$[C_4C_1Im][Tf_2N]$	0.31	0.045	0.55	−0.421	6.8
$[C_4C_1Im][Tf_2N]$	0.40	0.036	0.57	−0.421	6.9
$[C_4C_1Im][Tf_2N]$	0.44	0.035	0.56	−0.423	7.7
$[C_4C_1Im][Tf_2N]$	0.81	reversible		−0.424	10.6
$[C_4C_1Im][Tf_2N]$	∞	reversible		−0.425	18.9
$[C_6C_1Im][Tf_2N]$	0.36	0.020	0.54	−0.410	4.9
$[C_6C_1Im][Tf_2N]$	0.39	0.019	0.52	−0.411	5.1
$[C_6C_1Im][Tf_2N]$	0.47	0.016	0.53	−0.412	5.1
$[C_6C_1Im][Tf_2N]$	0.50	0.018	0.52	−0.412	6.1
$[C_6C_1Im][Tf_2N]$	0.92	reversible		−0.415	10.0
$[C_6C_1Im][Tf_2N]$	∞	reversible		−0.409	14.0
$[C_8C_1Im][Tf_2N]$	0.27	0.011	0.54	−0.403	2.5
$[C_8C_1Im][Tf_2N]$	0.30	0.013	0.52	−0.401	3.3
$[C_8C_1Im][Tf_2N]$	0.45	0.010	0.47	−0.403	3.8
$[C_8C_1Im][Tf_2N]$	0.73	0.011	0.54	−0.403	6.7
$[C_8C_1Im][Tf_2N]$	1.21	0.009	0.58	−0.401	9.1
$[C_8C_1Im][Tf_2N]$	∞	0.008	0.50	−0.405	6.7

[a] $\lambda' = k^0d/D$. λ at $L = \infty$ was calculated using the average k^0 value and $\lambda = k^0a/D$.

shows the responses obtained in $[C_2C_1Im][Tf_2N]$ and $[C_6C_1Im][Tf_2N]$ at a range of L values. Also shown in Figure 5 are the theoretical responses determined at each L value using eq 4. Very good fits were obtained in each case and, from these fits, best-fit values for $E^{0\prime}$, α, and k^0 were obtained. This procedure was repeated for each $[C_nC_1Im][Tf_2N]$ RTIL and the best fit parameters are shown in Table 4. In each RTIL, α was close to 0.5 and $E^{0\prime}$ was close to that estimated using cyclic voltammetry. The upper limit for measurable standard rate constants can be given in terms of the dimensionless parameter, $\lambda' = k^0d/D = Lk^0a/D$.[20] If $\lambda' \geq 10$, the tip voltammogram is essentially reversible. However, when the tip is positioned far from the substrate, the condition of reversibility is $\lambda = k^0a/D \geq 10$. Therefore, kinetic parameters in Table 4 were only determined from voltammograms that yielded $\lambda' < 10$. The average k^0 values were 0.078 ± 0.014, 0.039 ± 0.005, 0.018 ± 0.002, and 0.011 ± 0.001 cm s^{-1} in $[C_2C_1Im][Tf_2N]$, $[C_4C_1Im][Tf_2N]$, $[C_6C_1Im][Tf_2N]$, and $[C_8C_1Im][Tf_2N]$, respectively (errors are the standard deviations of four measurements of k^0). The deviation in the k^0 values obtained from the fits in each RTIL was quite low and there was no significant correlation between the tip-substrate distance and the values of k^0. These observations suggest that reliable kinetic measurements were obtained in these RTILs using SECM. In addition, Figure 6 shows the effect of positioning the tip close to the substrate on the voltammetric response and shows a normalized CV obtained when the tip was positioned close to the substrate ($L = 0.18$) in $[C_2C_1Im][Tf_2N]$, which is compared to that obtained when the tip was far from the substrate. The change in the shape of the CV when the tip was close to the substrate indicates that the tip response was governed by heterogeneous ET kinetics. Figure 7 shows the decrease in k^0 as the RTIL viscosity increased. Similar behavior to this has been observed for Fc and other redox mediators in conventional solvents as well as in RTILs.[41−43] The magnitudes of the k^0 values determined using this method are significantly lower than that measured for Fc oxidation in conventional solvent/electrolyte systems but are higher than those reported recently for Fc oxidation in RTILs. For example, Compton and co-workers recently reported a k^0 value of 7.5×10^{-3} and 6.0×10^{-3} cm s^{-1} for Fc in $[C_2C_1Im][Tf_2N]$ and $[C_4C_1Im][Tf_2N]$, respectively (using voltammetry).[37] Hapiot and co-workers reported values of 0.02 (using voltammetry) and 0.01 cm s^{-1} (using electrochemical

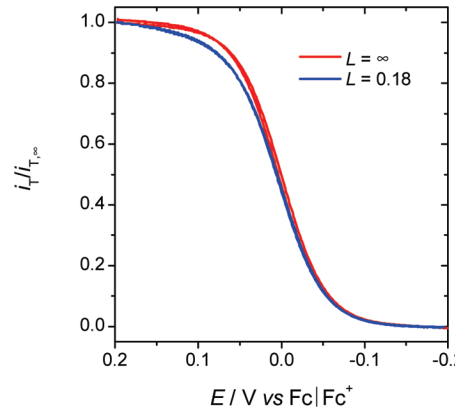

Figure 6. Normalized experimental SECM tip voltammograms obtained in 1.56 mM Fc dissolved in $[C_2C_1Im][Tf_2N]$ when the tip was located at a distance of $L = 0.18$ from the Pt substrate electrode (blue line) and when the tip was located far from the substrate electrode (red line). The substrate potential was held at −0.2 V vs $Fc|Fc^+$.

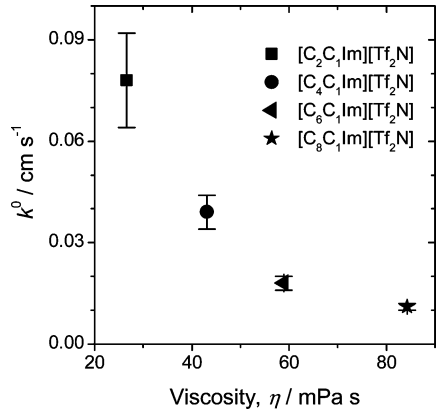

Figure 7. Graph of heterogeneous rate constant, k^0, vs viscosity for [C_nC_1Im][Tf_2N] RTILs, where $n = 2-8$. The error bars represent the standard deviation of four measurements of k^0.

impedance spectroscopy) for Fc in [C_2C_1Im][Tf_2N].[22] Our determination of higher k^0 values in RTILs using SECM is comparable to that of Mirkin and co-workers who measured higher rate constants for a number of redox couples using SECM than had previously been measured using voltammetry.[20] This confirms that (as has been suggested by others)[37] ohmic effects may be significant when performing kinetic measurements in RTILs using voltammetric methods. Therefore, steady-state SECM, which avoids problems associated with ohmic resistance, provides more accurate measurements of k^0 for redox couples in RTILs, as well as in aqueous and nonaqueous electrolytes. It is also interesting to note the difference in the rate constant measured for Fc oxidation using SECM and that determined for oxidation of the ferrocenylated RTIL [FcC_1C_1Im][Tf_2N]. We recently measured k^0 for oxidation of [FcC_1C_1Im][Tf_2N] when dissolved in [C_2C_1Im][Tf_2N] using SECM and k^0 was 7.6×10^{-3} cm s^{-1}.[29] This value is lower than that determined for Fc in this study. This phenomenon was also observed by Hapiot and co-workers, who measured lower rate constants for [FcC_1C_1Im][Tf_2N] oxidation in [C_2C_1Im][Tf_2N] than for Fc oxidation in [C_2C_1Im][Tf_2N].[22] The decrease in the rate constant on adding the imidazolium moiety to Fc could be due to the higher hydrodynamic radius in the ferrocenylated imidazolium salt, as has been observed in other Fc analogues.[44] However, as others have also indicated, such a dependence, which is derived from Marcus theory, is probably not applicable in RTILs as the solvent is composed completely of ions, whereas Marcus theory is based on the reorganization of solvent dipoles.[45] Therefore, before we can draw conclusions from such comparisons, further experimental and theoretical work is required to provide a thorough description of outer sphere electron transfer in RTILs.

Conclusions

The results described here demonstrate conclusively that it is possible to perform SECM in viscous RTILs, providing the experimental conditions are considered carefully. Using sufficiently small SECM tips and slow tip approach speeds, one can record SECM feedback approach curves that agree with conventional SECM theory in a range of RTILs. The Péclet number is a very useful guide for predicting whether feedback approach curves will agree with conventional SECM theory and, in the range $0.01 \leq Pe \leq 1.0$, convection effects cannot be neglected. The results reported here also have implications for the measurement of electron transfer kinetics in RTILs using conventional voltammetric methods. The k^0 values determined using SECM were higher than those determined recently for Fc oxidation in RTILs using cyclic voltammetry, suggesting that the use of conventional cyclic voltammetry for kinetic measurements in RTILs can lead to significant underestimations of k^0. Finally, we have shown here that the viscosity of RTILs has the same effect on k^0 as has been observed in other electrolytes, that is, k^0 decreases with increasing RTIL viscosity.

Acknowledgment. Financial support from the EPSRC under the Science and Innovation Award (DICE) is gratefully acknowledged (EP/D501229/1). P.L. is holder of an EPSRC Advanced Research Fellowship (EP/D073014/1).

Note Added after ASAP Publication. This paper was published ASAP on March 12, 2010. Text was revised in the last paragraph of the section entitled "Heterogeneous Electron Transfer Kinetics across the RTIL/Electrode Interface". The updated paper was reposted on March 17, 2010.

Supporting Information Available: Chronoamperometric data, graph of D_{Fc} versus $1/\eta$, and additional SECM feedback approach curve data. This material is available free of charge via the Internet at http://pubs.acs.org.

References and Notes

(1) de Souza, R. F.; Padilha, J. C.; Goncalves, R. S.; Dupont, J. *Electrochem. Commun.* **2003**, *5*, 728.
(2) Sekhon, S. S.; Lalia, B. S.; Park, J. S.; Kim, C. S.; Yamada, K. *J. Mater. Chem.* **2006**, *16*, 2256.
(3) Sakaebe, H.; Matsumoto, H. *Electrochem. Commun.* **2003**, *5*, 594.
(4) Garcia, B.; Lavallee, S.; Perron, G.; Michot, C.; Armand, M. *Electrochim. Acta* **2004**, *49*, 4583.
(5) Wang, P.; Zakeeruddin, S. M.; Moser, J. E.; Gratzel, M. *J. Phys. Chem. B* **2003**, *107*, 13280.
(6) Wang, P.; Zakeeruddin, S. M.; Comte, P.; Exnar, I.; Gratzel, M. *J. Am. Chem. Soc.* **2003**, *125*, 1166.
(7) Rogers, E. I.; Streeter, I.; Aldous, L.; Hardacre, C.; Compton, R. G. *J. Phys. Chem. C* **2008**, *112*, 10976.
(8) Barnes, A. S.; Rogers, E. I.; Streeter, I.; Aldous, L.; Hardacre, C.; Wildgoose, G. G.; Compton, R. G. *J. Phys. Chem. C* **2008**, *112*, 13709.
(9) Hagiwara, R.; Ito, Y. *J. Fluorine Chem.* **2000**, *105*, 221.
(10) Ohno, H. *Electrochemical Aspects of Ionic Liquids*; John Wiley & Sons: NJ, 2005.
(11) Shiddiky, M. J. A.; Torriero, A. A. J.; Zhao, C.; Burgar, I.; Kennedy, G.; Bond, A. M. *J. Am. Chem. Soc.* **2009**, *131*, 7976.
(12) Carano, M.; Bond, A. M. *Aust. J. Chem.* **2007**, *60*, 29.
(13) Buzzeo, M. C.; Klymenko, O. V.; Wadhawan, J. D.; Hardacre, C.; Seddon, K. R.; Compton, R. G. *J. Phys. Chem. A* **2003**, *107*, 8872.
(14) Armand, M.; Endres, F.; MacFarlane, D. R.; Ohno, H.; Scrosati, B. *Nat. Mater.* **2009**, *8*, 621.
(15) Macfarlane, D. R.; Forsyth, M.; Howlett, P. C.; Pringle, J. M.; Sun, J.; Annat, G.; Neil, W.; Izgorodina, E. I. *Acc. Chem. Res.* **2007**, *40*, 1165.
(16) Laforge, F. O.; Velmurugan, J.; Wang, Y. X.; Mirkin, M. V. *Anal. Chem.* **2009**, *81*, 3143.
(17) Laforge, F. O.; Kakiuchi, T.; Shigematsu, F.; Mirkin, M. V. *Langmuir* **2006**, *22*, 10705.
(18) Bard, A. J.; Mirkin, M. V. *Scanning Electrochemical Microscopy*; Marcel Dekker: New York, 2001.
(19) Sun, P.; Laforge, F. O.; Mirkin, M. V. *Phys. Chem. Chem. Phys.* **2007**, *9*, 802.
(20) Sun, P.; Mirkin, M. V. *Anal. Chem.* **2006**, *78*, 6526.
(21) Nkuku, C. A.; LeSuer, R. J. *J. Phys. Chem. B* **2007**, *111*, 13271.
(22) Fontaine, O.; Lagrost, C.; Ghilane, J.; Martin, P.; Trippe, G.; Fave, C.; Lacroix, J. C.; Hapiot, P.; Randriamahazaka, H. N. *J. Electroanal. Chem.* **2009**, *632*, 88.
(23) Zigah, D.; Ghilane, J.; Lagrost, C.; Hapiot, P. *J. Phys. Chem. B* **2008**, *112*, 14952.
(24) Zigah, D.; Wang, A. F.; Lagrost, C.; Hapiot, P. *J. Phys. Chem. B* **2009**, *113*, 2019.
(25) Holbrey, J. D.; Reichert, W. M.; Swatloski, R. P.; Broker, G. A.; Pitner, W. R.; Seddon, K. R.; Rogers, R. D. *Green Chem.* **2002**, *4*, 407.
(26) Bonhote, P.; Dias, A. P.; Papageorgiou, N.; Kalyanasundaram, K.; Gratzel, M. *Inorg. Chem.* **1996**, *35*, 1168.

(27) Snook, G. A.; Best, A. S.; Pandolfo, A. G.; Hollenkamp, A. F. *Electrochem. Commun.* **2006**, *8*, 1405.
(28) Bard, A. J. In *Scanning Electrochemical Microscopy*; Bard, A. J., Mirkin, M. V., Eds.; Marcel Dekker: New York, 2001.
(29) Taylor, A. W.; Qiu, F. L.; Hu, J. P.; Licence, P.; Walsh, D. A. *J. Phys. Chem. B* **2008**, *112*, 13292.
(30) Tokuda, H.; Tsuzuki, S.; Susan, M.; Hayamizu, K.; Watanabe, M. *J. Phys. Chem. B* **2006**, *110*, 19593.
(31) Fitchett, B. D.; Knepp, T. N.; Conboy, J. C. *J. Electrochem. Soc.* **2004**, *151*, E219.
(32) Rogers, E. L.; Silvester, D. S.; Poole, D. L.; Aldous, L.; Hardacre, C.; Compton, R. G. *J. Phys. Chem. C* **2008**, *112*, 2729.
(33) Huang, X. J.; Rogers, E. I.; Hardacre, C.; Compton, R. G. *J. Phys. Chem. B* **2009**, *113*, 8953.
(34) Bond, A. M.; Colton, R.; Harvey, J.; Hutton, R. S. *J. Electroanal. Chem.* **1997**, *426*, 145.
(35) Buzzeo, M. C.; Evans, R. G.; Compton, R. G. *ChemPhysChem* **2004**, *5*, 1106.
(36) Amphlett, J. L.; Denuault, G. *J. Phys. Chem. B* **1998**, *102*, 9946.
(37) Barnes, A. S.; Rogers, E. I.; Streeter, I.; Aldous, L.; Hardacre, C.; Compton, R. G. *J. Phys. Chem. B* **2008**, *112*, 7560.
(38) Doherty, A. P.; Brooks, C. A. *Electrochim. Acta* **2004**, *49*, 3821.
(39) Mirkin, M. V., In *Handbook of Electrochemistry*; Zoski, C. G., Ed.; Elsevier: Amsterdam, 2007.
(40) Velmurugan, J.; Sun, P.; Mirkin, M. V. *J. Phys. Chem. C* **2009**, *113*, 459.
(41) Miao, W. J.; Ding, Z. F.; Bard, A. J. *J. Phys. Chem. B* **2002**, *106*, 1392.
(42) Zhang, X.; Yang, H.; Bard, A. J. *J. Am. Chem. Soc.* **1987**, *109*, 1916.
(43) Karpinski, Z. J.; Song, S.; Osteryoung, R. A. *Inorg. Chim. Acta* **1994**, *225*, 9.
(44) Clegg, A. D.; Rees, N. V.; Klymenko, O. V.; Coles, B. A.; Compton, R. G. *J. Electroanal. Chem.* **2005**, *580*, 78.
(45) Fietkau, N.; Clegg, A. D.; Evans, R. G.; Villagran, C.; Hardacre, C.; Compton, R. G. *ChemPhysChem* **2006**, *7*, 1041.

JP912087N